



OPEN Evaluation of chip breaker designs on tool life and hole integrity in drilling of HFRP/Al composite

Muhammad Zubair Afzal^{1,2}, Sarmad Ali Khan¹, Muhammad Umar Farooq³✉, Atif Javaid⁴, Saqib Anwar⁵ & Adeolu A. Adediran^{6,7}✉

In this study, drilling of a newly developed lightweight fire-retardant carbon/glass-fiber-reinforced polymer epoxy sandwich that includes an aluminum honeycomb core with modified epoxy (HFRP/Al sandwich composite) is investigated. A new high-performance insert combination comprising central-stepped and peripheral-wiper inserts is evaluated. The geometry of the central insert is kept constant while two variations in chip breaker (C_b) designs are introduced on wiper inserts differentiated mainly based on C_b width and C_b depth. Variation one abbreviated as LM geometry has a C_b depth of 65 μm and a C_b width of 1000 μm while the second variation terms as GT geometry has a C_b depth of 20 μm and a C_b width of 720 μm . This study is conducted in two phases at a constant speed (CS) of 50 m/min in a dry-cutting environment. Phase I involved four tests, in each test ten holes are drilled with LM and GT geometries at two different feed rates (0.08 and 0.16 mm/rev). Based on reduced diametric error, and delamination, tests with a feed rate (FR) of 0.08 mm/rev are selected for Phase-II analysis, which involves the evaluation of tool life testing. The results in terms of tool life, diametric error, and delamination factors are reported. Notably, the GT geometry of the wiper inserts outperformed the LM geometry in terms of 33% higher tool life compared to its LM counterpart. In addition, the diametric error and delamination factor are substantially lower with the former geometry in comparison to the latter one. The better performance of GT geometry is attributed to its better chip flow and robust design.

Keywords Drilling, HFRP, Wiper insert, Flank wear, Diametric error

The development of hybrid fiber-reinforced polymers (HFRPs) has increased in recent years. These hybrid composites offer low density, high strength, excellent elongation, superior corrosion resistance, and cost-effectiveness¹. Due to this, usage of HFRPs is being increased in automotive, aerospace, railways, and power generation industries. In particular, components such as wind turbine blades and drive shafts have benefited from the exceptional mechanical performance and durability of HFRPs². CFRP/metal stacks are commonly joined using mechanical fastening methods, such as rivets and bolts, which require a large number of drilled holes for complete assembly, often necessitating thousands of holes. For illustration, the manufacturing process of the Airbus A350 aircraft (which includes large CFRP composite components) requires approximately 55,000 holes³. Drilling of CFRP/metal stacks poses a significant challenge because of the disparate machinability characteristics of the individual materials involved. Consequently, a variety of defects frequently arise during the assembly process, thereby significantly compromising the precision. It is also worth mentioning that the quality of the holes has a direct impact on the durability of the aircraft, as previous data indicate that rejections of up to 60% are caused by faulty holes⁴. Thus, the industry faces significant challenges in achieving good quality machining of CFRP/metal composites owing to the distinct properties of carbon fibers and metals⁵. The process of drilling composite structures can result in significant issues such as the formation of critical defects in drilled

¹Department of Industrial and Manufacturing Engineering, University of Engineering and Technology, Lahore 54890, Pakistan. ²Department of Mechanical Engineering, NFC Institute of Engineering and Fertilizer Research, Faisalabad, Pakistan. ³School of Mechanical Engineering, University of Leeds, Leeds LS2 9JT, UK. ⁴Department of Polymer and Process Engineering, University of Engineering and Technology, G. T. Road, Lahore 54890, Pakistan. ⁵Industrial Engineering Department, College of Engineering, King Saud University, Riyadh 11421, Saudi Arabia. ⁶Department of Mechanical Engineering Science, University of Johannesburg, Johannesburg, South Africa. ⁷Materials and Metallurgical Engineering Department, Federal University Oye-Ekiti, Oye-Ekiti, Ekiti State, Nigeria. ✉email: umarmuf0@gmail.com; dladesoji@gmail.com

holes. These defects may include delamination of the CFRP, burrs in both materials, and potential damage to the stack interface due to mechanical and thermal loading⁶.

According to the study conducted by Braiek et al.⁷ investigated the drilling performance of E-glass-reinforced vinylester (VE411) hybrid composite tubes using 6 mm TiAlN-coated and diamond-coated solid carbide drills. Experiments were performed at cutting speeds of 1000, 2000, and 3000 rpm, with feed rates ranging from 0.05 to 0.40 mm/rev. The findings indicate that an increase in the feed rate resulted in a higher surface roughness (Ra) and a greater delamination factor (Fd). Optical analysis revealed that delamination occurred exclusively at the hole entry point (mechanical layer) of the hybrid composite tube. Boughdiri et al.⁸ experimentally validated the FE simulation for drilling GLARE, showing good correlation with experimental results. However, the model has limitations because it does not account for the thermal effects on the mechanical properties. Elevated cutting temperatures can exceed the glass transition temperature of glass-epoxy layers, reducing their mechanical properties and impacting the residual stresses in the laminate. Sourd et al.⁹ evaluated the drilling of a GLARE fiber metal using abrasive water jets, focusing on damage and contamination. The results showed negligible influence of drilling parameters on the hole wall surface roughness, with a maximum roughness below 6 μm , which is comparable to conventional drilling. A high water pressure improved the hole cylindricity and achieved the target diameter. Ge et al.¹⁰ assessed the hole-making performance of thermoplastic CF/PEKK composites by comparing conventional drilling and helical milling at various feed rates. Results indicated that conventional drilling at low feed rates (0.1 mm/rev) generated high machining temperatures, while helical milling produced even higher temperatures, exacerbating delamination damage. Microstructural analysis revealed matrix smearing on all the hole surfaces owing to the in-plane shear stress and elevated temperatures. Ge et al.¹¹ presents a hybrid optimization approach combining NSGA-II and TOPSIS to identify Pareto solutions for thermoplastic CF/PEKK drilling, with a focus on sustainable manufacturing. This study compares the effects of matrix properties on the optimization outcomes by comparing CF/PEKK with conventional CF/epoxy composites. The experimental results demonstrate that the proposed method achieves 91.5–95.7% prediction accuracy, effectively controlling delamination and thermal damage within permissible limits. Ge, Tan, et al.¹² investigated the cutting physics in orthogonal cutting of carbon fiber-reinforced thermoplastic (CFRTP) composites, considering three cutting temperatures (23 °C, 100 °C, and 200 °C) and four fiber orientations (0°, 45°, 90°, and 135°). Using a microscale finite element analysis (FEA) model, the study highlighted the transition in cutting behavior with temperature, particularly beyond the glass transition temperature, where thermal softening of the matrix and degradation of interface bonding and fracture toughness occur. According to Ge, Luo, et al.¹³, this study is the first to reveal the evolution of machining temperatures during the drilling of CF/PEKK and their impact on material damage. A comparative analysis of CF/epoxy highlights the differences in drilling performance linked to their thermal and mechanical properties. The ductility and thermal sensitivity of CF/PEKK resulted in continuous chip formation, whereas the brittleness of CF/epoxy led to segmented chips. Sharma et al.¹⁴, the tensile behavior of FMLs comprising aluminum 2024-T3 sheets (0.2, 0.4, 0.6 mm thick) and unidirectional glass-fiber composites was analyzed. Although the layup sequence did not affect the initial modulus, it significantly influenced the ultimate strength and post-ultimate strength behavior.

The inadequate fire-retardant properties of HFRP composites pose a significant challenge for structural applications^{15,16}. The consequences of structural deterioration in composites due to heat exposure during and after a fire incident can have serious implications for the well-being of firefighters, integrity of load-bearing structures, and safety of building occupants. Recently, a sandwich panel with fire-retardant properties was fabricated using the contact molding technique with an aluminum honeycomb core between the layers of glass and carbon fiber¹⁷. However, drilling of this significant newly developed HFRP/Al sandwich composite has not yet been evaluated. Previously, solid carbide drills were the only option for drilling operations¹⁸. Recently, tool manufacturers have developed a combination of peripheral wiper insert and central stepped insert for drilling applications. This combination was evaluated in previous studies, in which the drilling of superalloys such as Inconel 718 and Ti-6Al-4 V were tested. This tooling combination outperformed conventional tooling^{19–21}. Though the results of this insert combination were promising for superalloys but suitability of these novel insert combination has remained unexplored in composites drilling generally and fire retardant HFRPs particularly²¹. The promising results in previous studies motivated the authors to evaluate this tooling configuration on this newly developed HFRP/Al sandwich composite. In this study, a center-stepped insert with a peripheral wiper insert was used to drill a newly fabricated fire-retardant HFRP/Al sandwich composite. Output responses involving tool life, diametric error, and delamination factor were taken into account.

Experimental work

Materials

Polyacrylonitrile (PAN)-based plain weave carbon fibers and plain weave glass fiber mats were procured from Easy Composites, Staffordshire, UK. The matrix material comprised diglycidyl ether of bisphenol A (DGEBA) epoxy, supplied by Kukdo Chemical Co., Ltd., Seoul, South Korea, and cross-linked with triethylenetetramine, sourced from Sigma Aldrich, Dorset, UK. Ammonium polyphosphate (APP) with a phosphorous content of 29%, particle size ranging from 18 to 22 μm , was obtained from Shifang Changfeng Chemical Co., Ltd., Deyang, China, and utilized as a fire-retardant additive. Additionally, perforated corrosion-treated aluminum honeycomb, featuring a 1.91 cm cell size, 2 cm core thickness, and 50 μm foil thickness (3003 aluminum alloy), was also purchased from Easy Composites, Staffordshire, UK, and employed as the core material for fabricating sandwich composites. In depth detail about the material presented in previous study¹⁷.

Fabrication of sandwich composites

The HFRP/Al sandwich composite was fabricated using a contact molding technique. To enhance the fire-retardant properties of the carbon and glass fibers, their surfaces were pre-treated with phosphoric acid prior to the fabrication process. The composite structure, with dimensions of $260 \times 260 \times 23$ mm, was constructed by incorporating a honeycomb core made of 3003 aluminum alloy. This core was sandwiched between eight layers of carbon fiber and a single layer of glass fiber from above and below, as illustrated in Fig. 1a. The assembly was impregnated with a diglycidyl ether of bisphenol A (DGEBA) epoxy resin. To further enhance fire resistance, ammonium polyphosphate (APP) was added to the DGEBA epoxy resin at a concentration of 10% by weight. The carbon and glass fiber reinforcements, along with the aluminum honeycomb core, were impregnated with the resin mixture using a roller to ensure uniform distribution. The final composite structure, depicted in Fig. 1b, underwent a curing process at 30°C for 20 h, followed by post-curing at 80°C for 1 h to achieve optimal material properties. Specific details regarding the mechanical properties, thermal behavior, and flexural properties have been documented in a previous study¹⁷.

Cutting tools

A tool holder made in Sweden by Sandvik Coromant with usable length of 28.32 mm and drill diameter (DC) of 14 mm was used in the drilling of HFRP/Al sandwich composite. This specific type of tool holder holds two inserts for drilling purpose, one insert at the center of tool and other at the periphery of drill as shown in Fig. 2a. The central insert used in this study has a stepped technology with a rake angle of 18° . Both the cutting edge of central insert features steps behind the edge, thereby decreasing the level of engagement of cutting edges compared to conventional drilling inserts. The step technology which is illustrated in Fig. 2b, is taken from reference²². In addition, the peripheral insert used in this study has a wiper edge technology with a rake angle of 10° . Conventional cutting tools are known to produce peaks on the machined surface. However, wiper inserts offer a solution to this issue by utilizing the radii on the tool nose. This design allows for longer contact with the workpiece, resulting in reducing the peaks. This process is referred to as “wiper,” which has led to the development of the “wiper insert”. Both inserts were coated with Titanium-Aluminum-Nitride (TiAlN) using a physical vapor deposition (PVD) method.

Two different peripheral-wiper insert chip breakers (C_B) abbreviated as LM and GT, were used to drill an HFRP/Al sandwich composite. Both inserts have groove-type C_B . Groove-type C_B helps in chip breaking by the curling of chips. The accumulation of chips that do not break away from the tool-workpiece can have a detrimental impact on several aspects of the machining process, including surface finish, operator safety, work accuracy, tool life, machine vibrations, and overall performance^{23,24}. General terminologies of C_B are depicted in Fig. 2c. Therefore, it is important to evaluate the C_B designs of wiper inserts. The detailed geometries of the C_B used in this study were measured by cutting the inserts into cross-section using EDM machine and then using a coordinate measuring machine (CMM). The details of C_B are presented in Table 1. The comparison between the LM and GT geometries reveals differences in several aspects, such as C_B depth and width, wedge angle, and rake angle. While the LM geometry displays a higher C_B depth and width, as well as a smaller wedge angle and greater rake angle, the GT geometry exhibits a smaller C_B width and height, a higher wedge angle, and a smaller rake angle. These disparities lead to a weaker LM geometry, as its greater positive rake angle contrasts with the GT geometry's smaller positive rake angle and more robust design for rigid material like HFRP/Al sandwich composites.

Experimentation details

The experiments were carried out in two phases, using a constant cutting speed (CS) of 50 m/min and two feed rates (FR) of 0.08 and 0.16 mm/rev, on a CNC machining center. The CNC machining center used was the First MCV-600 machining center by Long Chang Machinery Co Ltd., which has three axes, 15 horsepower, and 8000 top RPM. The drilling setup is represented in Fig. 3. Phase I of the study employed a full factorial design to conduct four experiments under dry drilling conditions. To assess repeatability, Tests 3 and 4 were repeated (identified as Tests 3R and 4R). The input parameters and full factorial design of the experiment are presented

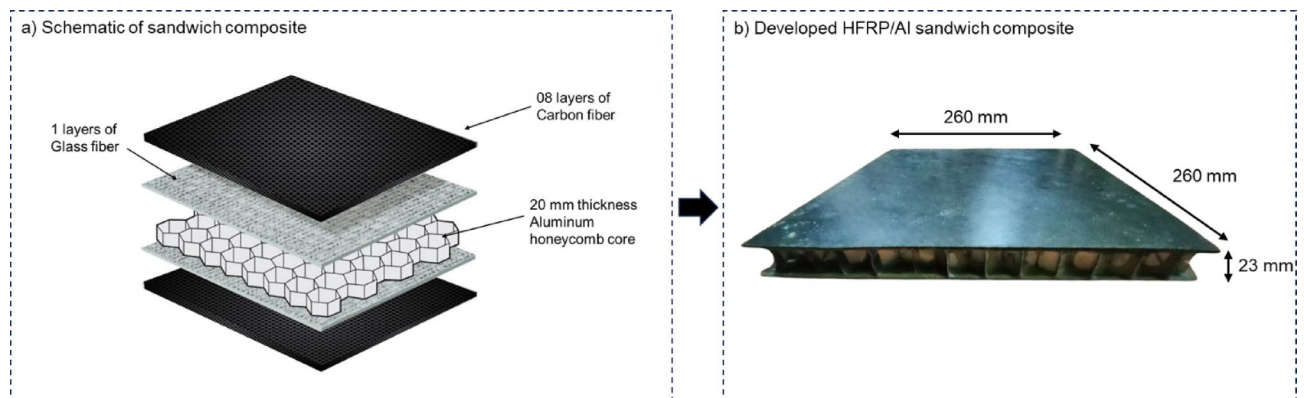


Fig. 1. (a) Schematic of sandwich composite (b) Developed HFRP/Al sandwich composite.

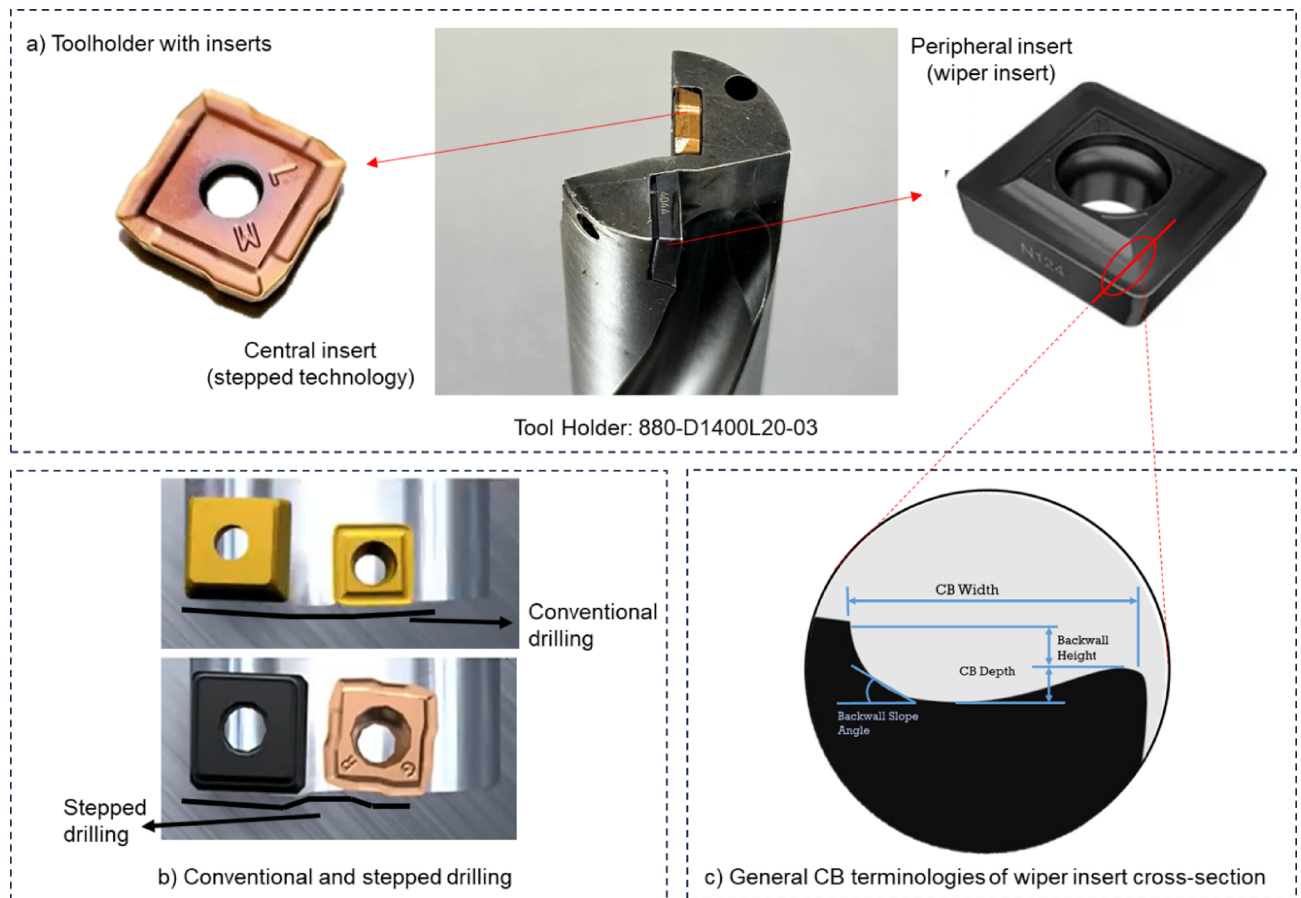


Fig. 2. (a) Tool holder with central and peripheral insert, (b) conventional and stepped insert drilling (c) generalized chip breaker terminologies.

| Chip breaker (C_B) | LM | GT |
|---------------------------------------|------|-----|
| Depth of C_B (μm) | 65 | 20 |
| Width of C_B (μm) | 1000 | 720 |
| Height of Back wall (μm) | 145 | 120 |
| Angle of Back wall slope | 30° | 27° |

Table 1. Details of wiper insert chip-breakers.

in Tables 2 and 3, respectively. Due to the limited quantity of newly developed fire retardant HFRP/Al sandwich composites, ten holes were drilled for each experiment in Phase 1. Tool wear measurements and optical images of inserts during the drilling process were taken using a coordinate measuring machine (CMM), equipped with a digital camera of 70 × magnification using Quadra check (QC)-5000 software (<https://cmmtechnology.com/quadra-check-5000-cmm-measuring-software/>). The diametric error, which is the discrepancy between the actual value and the DC value²⁵, was evaluated using the CMM. In Phase II experimentation, two tests were conducted on the basis of lower diametric errors and observation of a smaller delamination factor from Phase I and these tests were extended to the tool life criterion, which was set at 150 μm ²⁶. The detailed diametric error and delamination factor were assessed over the tool life duration using CMM. Babu et al.,²⁷ introduced a delamination factor (F_d) to evaluate and compare the degree of delamination resulting from drilling composites, which is defined as the ratio of the maximum diameter of delamination (D_{max}) to the nominal diameter of the drilled hole (D_{nom}) was calculated using the formula given in Eq. (1):

$$F_d = \frac{D_{\text{max}}}{D_{\text{nom}}} \quad (1)$$

Moreover, the tool-wear mechanisms of cutting inserts were examined using SEM.

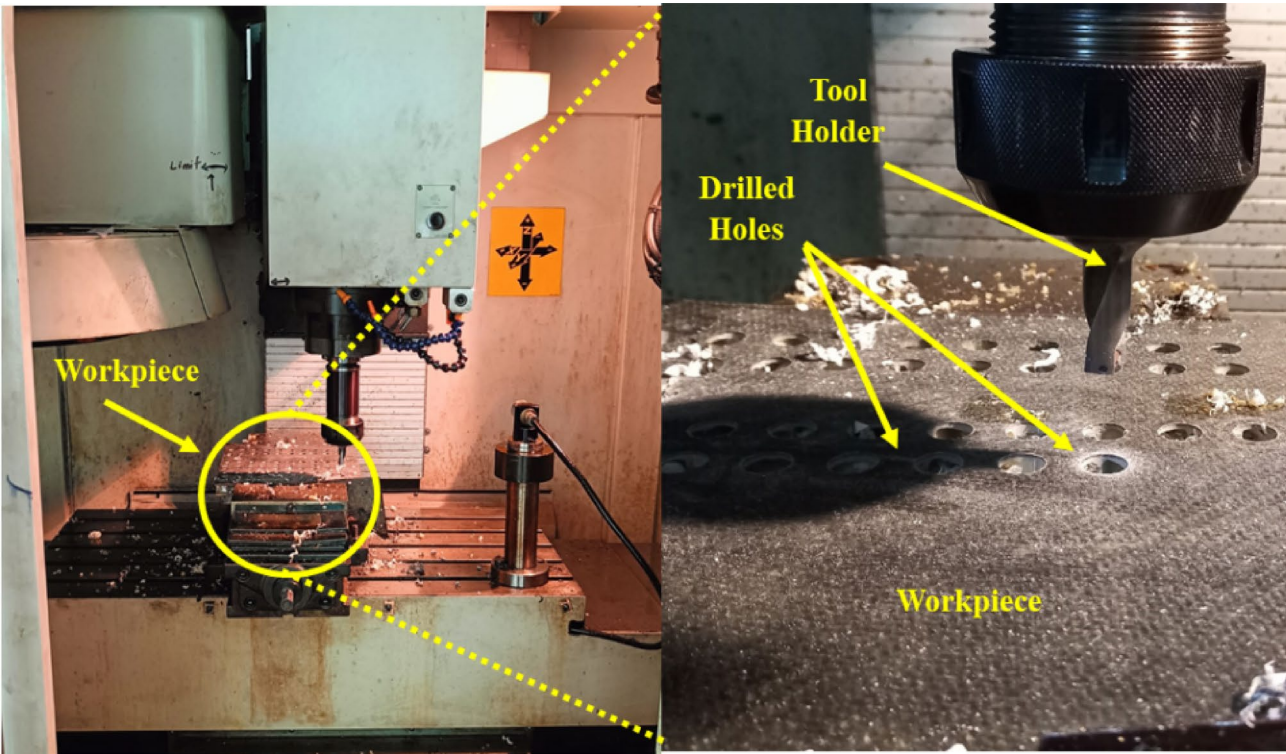


Fig. 3. Experimental setup.

| Parameters | Levels | |
|-------------------------|--------|------|
| | L-1 | L-2 |
| Wiper insert geometry | LM | GT |
| Feed rate - FR (mm/rev) | 0.08 | 0.16 |

Table 2. Level of input parameters.

| | Test # | Geometry | Feed rate (mm/rev) |
|--------------------------------------------------|--------|----------|--------------------|
| Phase-I | 1 | GT | 0.08 |
| | 2 | GT | 0.16 |
| | 3 | LM | 0.08 |
| | 4 | LM | 0.16 |
| | 3R | LM | 0.08 |
| | 4R | LM | 0.16 |
| Phase-II | 1E | GT | 0.08 |
| | 3E | LM | 0.08 |
| R indicates repeated tests | | | |
| E indicates extended tests to tool life criteria | | | |

Table 3. Full factorial design of experiments.

Results and discussions
Tool wear

The relationship between the number of hole and flank wear is shown in Fig. 4. Ten holes were drilled in each experiment to evaluate the tool wear trend, and no significant difference was observed in either geometry. In general, an increase in the tool wear was observed with an increase in the number of drilled holes. GT geometry exhibited lower tool wear than the LM geometry. A minimum flank wear of 50 μm was observed in Test 1 using GT geometry with a FR of 0.08 mm/rev. The flank wear curves for all tests were steady owing to the uniform wear. Marginally higher flank wear was observed for a higher FR of 0.16 mm/rev for all tests. The maximum tool

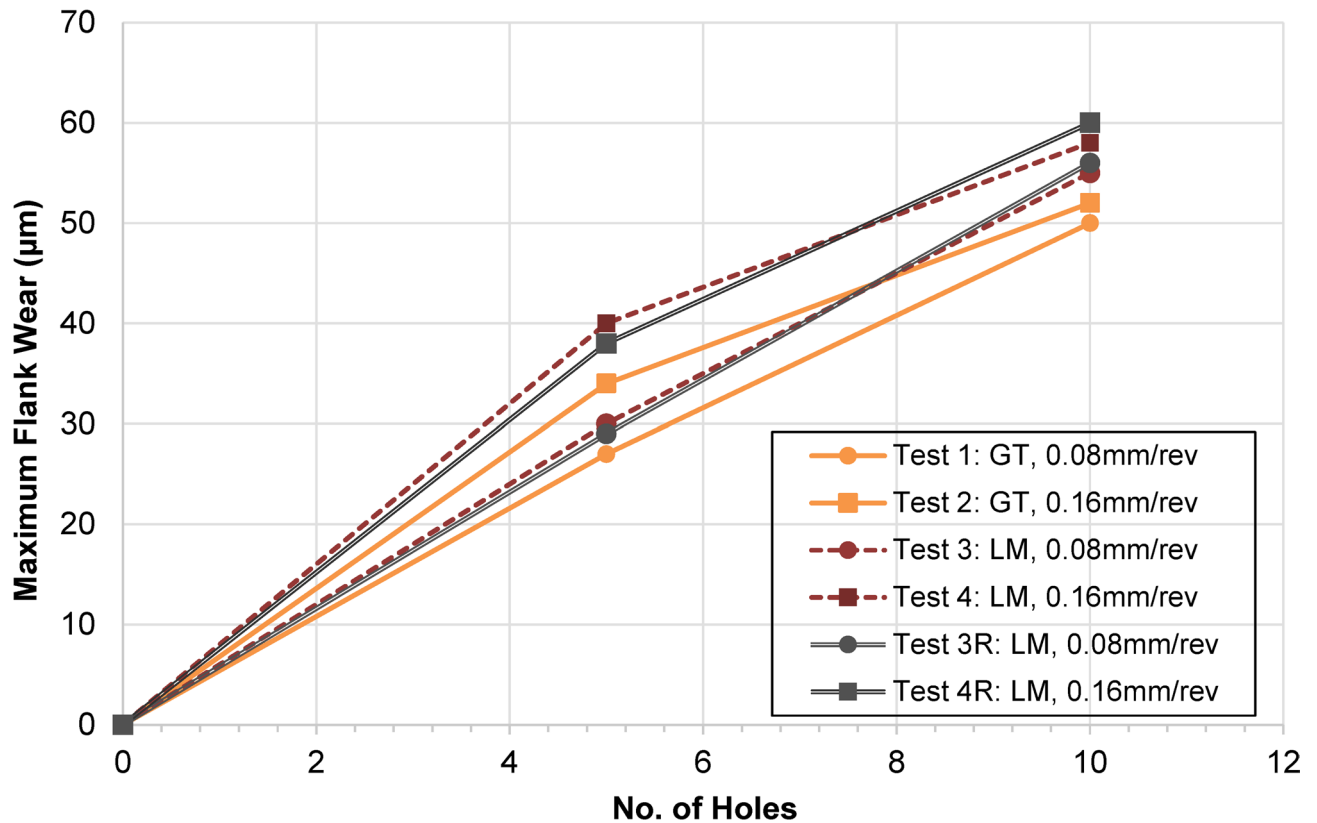


Fig. 4. Tool wear Vs No of Holes.

wear of 60 μm was observed in Test 4 for the LM geometry at FR of 0.16 mm/rev. Compared to the LM geometry, the GT geometry displayed approximately 15% less tool wear at a maximum FR of 0.16 mm/rev. The basic aim for drilling ten holes was to observe the delamination and diametric error.

The main effect plots show both the factors significant for the tool wear as shown in Fig. 5 using Minitab 17 available at <https://www.minitab.com/en-us/products/minitab>.

Diametric error

Tight geometric and dimensional tolerances are critical in the assembly of composite materials, especially in the aerospace industry, where accuracy is paramount²⁸. In an effort to examine the impact of wiper insert geometry and FR on the diameter discrepancy, the diameter of the drilled holes at three separate locations were measured. The average values of the measurements are reported herein. Figure 6 shows the diametric error with respect to the number of drilled holes. All the tests consistently exhibited positive diametric errors. This indicates that the diameters of the drilled holes were consistently higher than the specified nominal diameter. The results indicated that the lower FR of 0.08 mm/rev exhibited a lower diametric error. Moreover, in all experiments, it was observed that the diametric error exhibited a downward trend with an increasing number of holes owing to the lower corner wear. Overall, LM geometry exhibits a lower diametric error due to higher tool wear compared to GT geometry. For the 10th hole at both the FR , LM geometry resulted in a diametric error of 60 μm compared to 70 μm in the case of GT geometry. The results showed that FR had a marginal impact on the diametric error. The higher level of FR (0.16 mm/rev) resulted in a greater diametric error due to higher vibrations²⁹.

Hole integrity analysis

Hole images were taken from the top and bottom using a digital camera for all tests to observe the overall delamination, as shown in Figs. 7 and 8, respectively. The entrance of the holes displayed minimal or no delamination, a phenomenon referred to as pull-up delamination, whereas greater delamination is observed at the exit of the holes, which is also known as push-out delamination. Delamination, including burrs and tears, appeared on the exist side of the holes. A marginally higher delamination was observed at a higher FR of 0.16 mm/rev. Similar results were obtained by³⁰, where a higher delamination factor was observed at higher CS and FR . Durão et al.³¹ proposed a method for selecting FR . The researchers carried out drilling experiments with CFRP using three distinct geometric shapes for the drill bits. The findings reveal that irrespective of the type of drill bit employed, a greater FR leads to more serious delamination because at a higher FR , the drill cutting edge operates similar to a punch, leading to an increase in linear extrusion speed and a transfer of additional energy to the uncut piles. Consequently, it is imperative to minimize the FR to prevent severe delamination along the periphery of the drilled hole. In addition, an increase in the FR increases the chip thickness (higher thrust

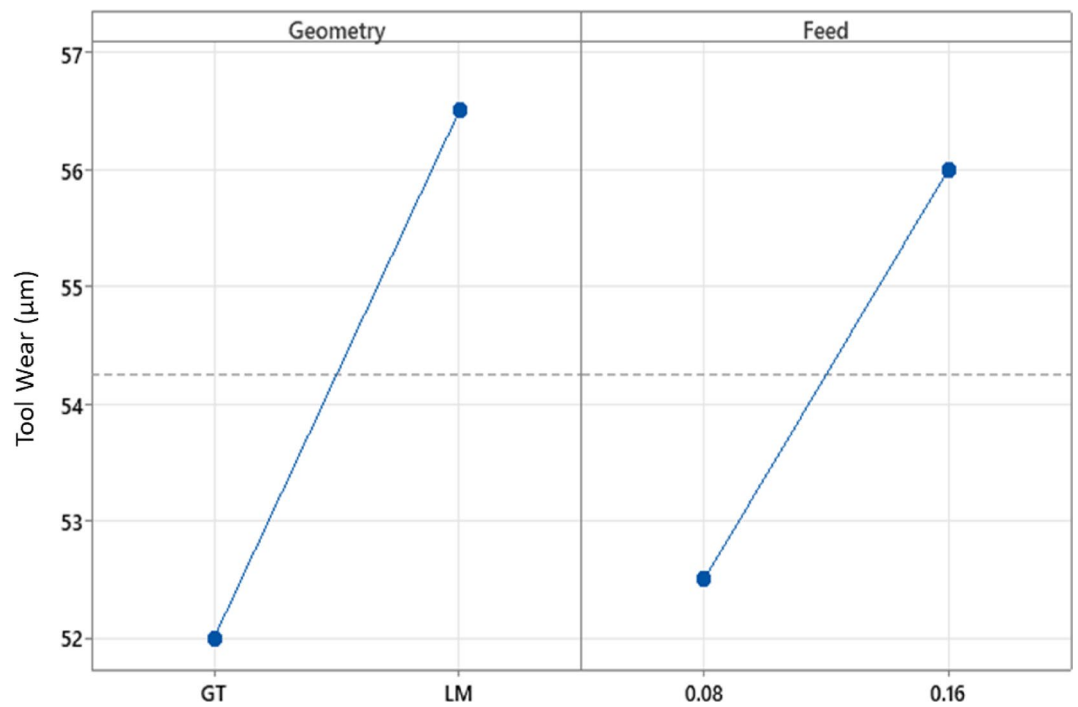


Fig. 5. Main effect plot for tool wear.

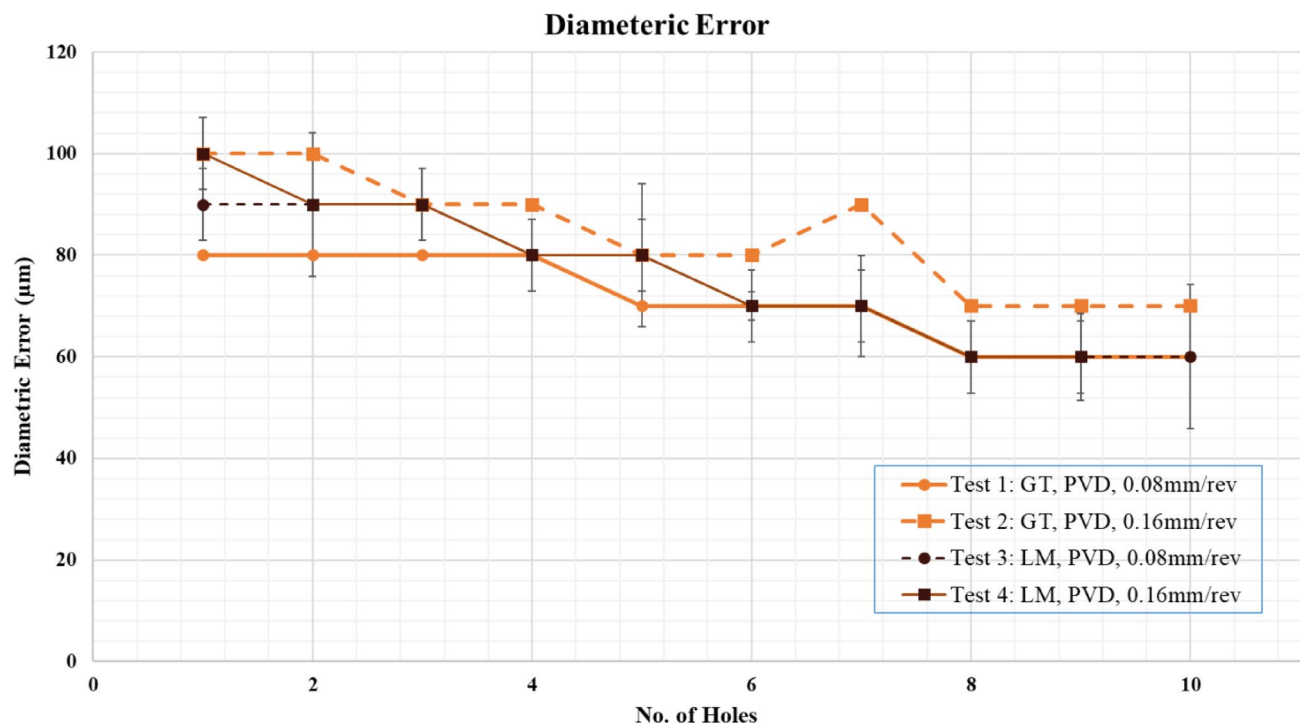


Fig. 6. Diametric error vs. no. of holes.

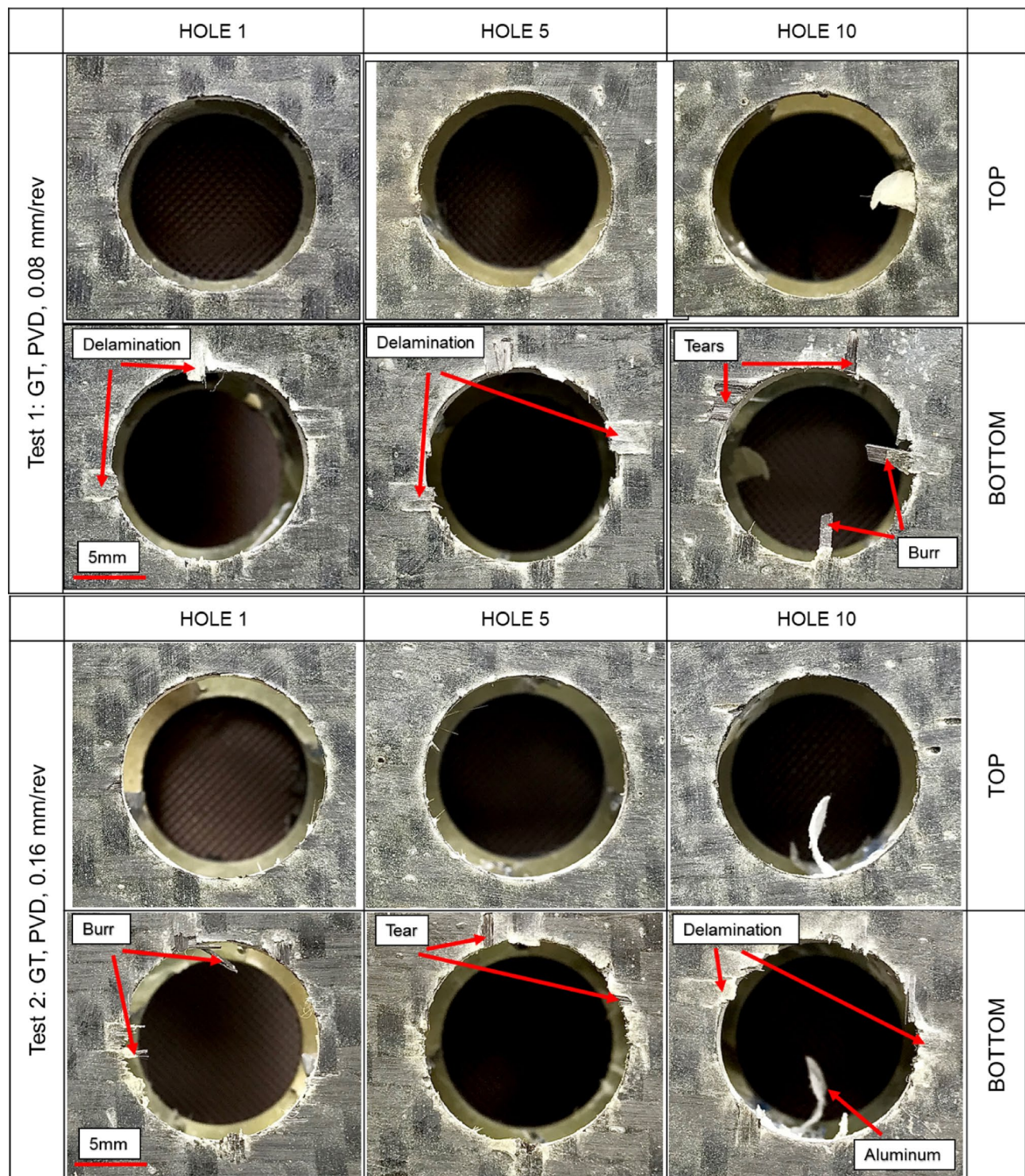


Fig. 7. Drilled hole images of top and bottom for Tests 1 and 2.

force) between the workpiece and tool, producing a violent fracture, which leads to high delamination. However, regardless of the geometry, the diametric error and delamination at the bottom of the hole were lower at lower *FR* of 0.08 mm/rev. Consequently, Tests 1 and 3 (lower *FR*) from phase I were selected for further evaluation.

Phase-II: tool life testing and associated hole integrity

Tests 1 and 3 were analyzed in further detail to meet the 150 μ m maximum tool life criterion as Tests 1E and 3E. Figure 9 shows the flank wear and the number of drilled holes. In Test 3E, total number of 90 holes were drilled

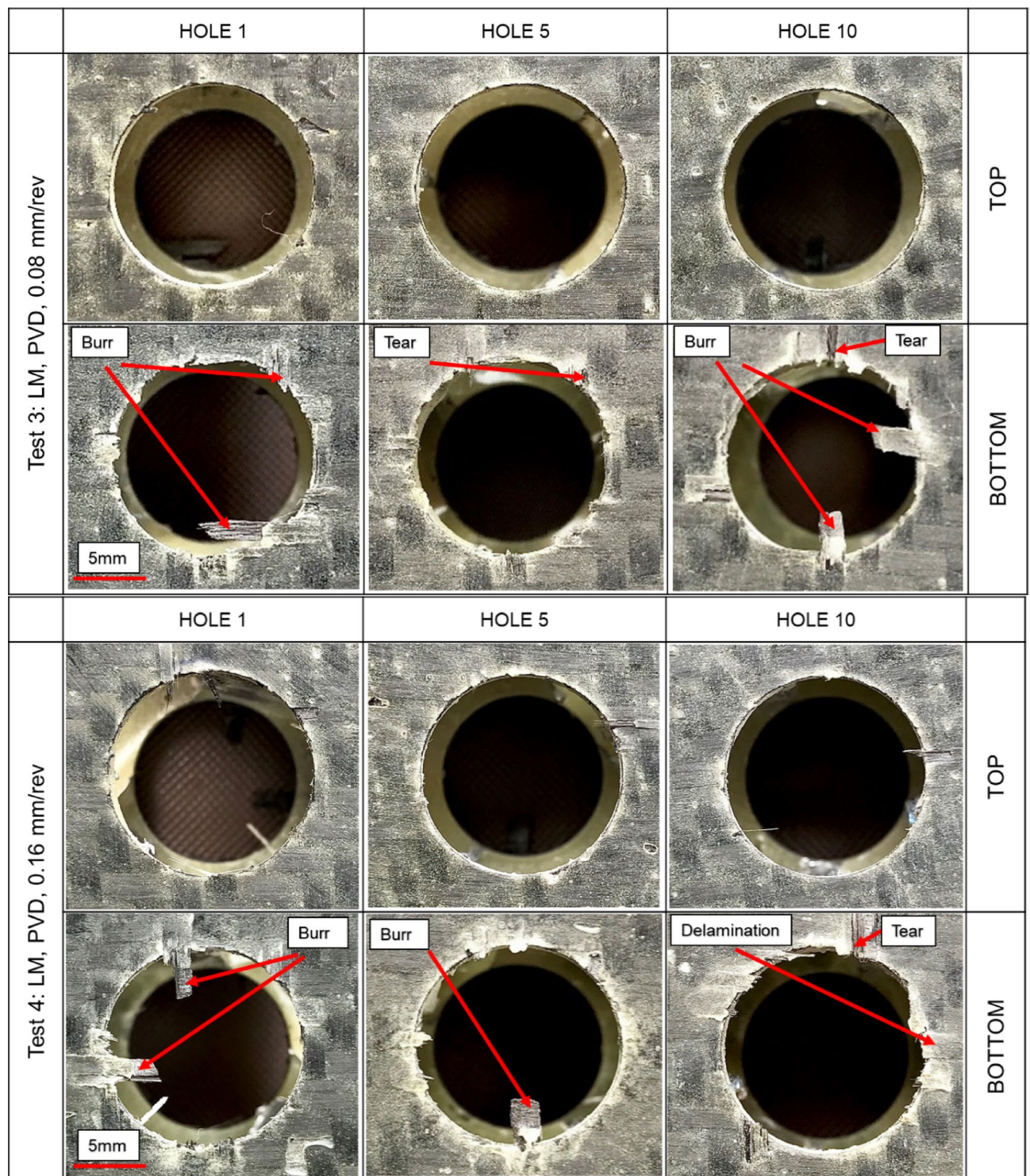


Fig. 8. Drilled hole images of top and bottom for Tests 3 and 4.

using LM geometry whereas a maximum of 120 holes were drilled using GT geometry in Tests 1E. The results demonstrated that the GT geometry exhibited a 33% improvement in tool life relative to the LM geometry.

This can be attributed to the fact that the HFRP/Al sandwich composite with glass fiber, carbon fiber, and resin constitutes a very rigid combination of materials that cannot easily flow over the tool geometry. Therefore, a more aggressive flow condition such as a steeper angle and deeper C_b width imparted on LM geometry leads to difficult chip flow conditions for the HFRP/Al sandwich composites which in turn increased the cutting forces at the tool-chip interface generating greater thermo-mechanical effects on the tool wear. Moreover, these chips come in contact between the tool and hole wall, thereby increasing the flank wear and reducing the

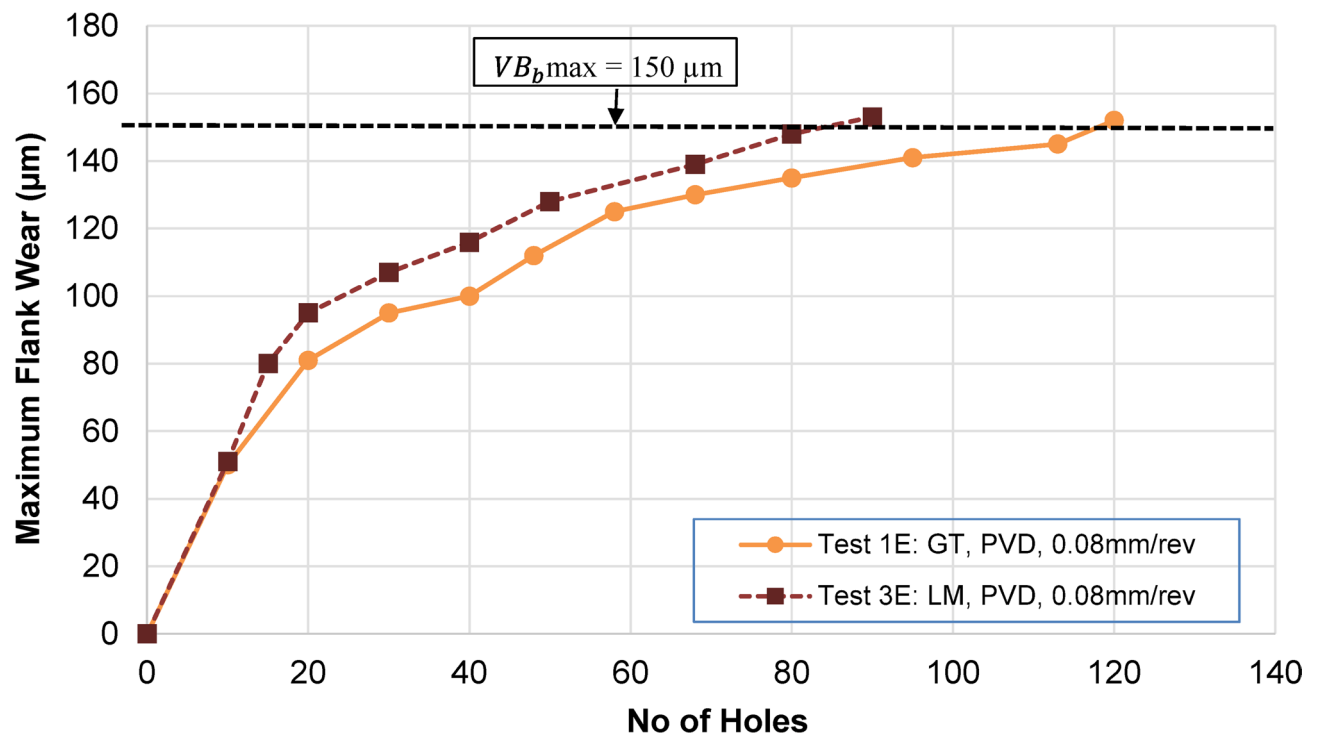


Fig. 9. Maximum Flank wear vs. No. of Holes.

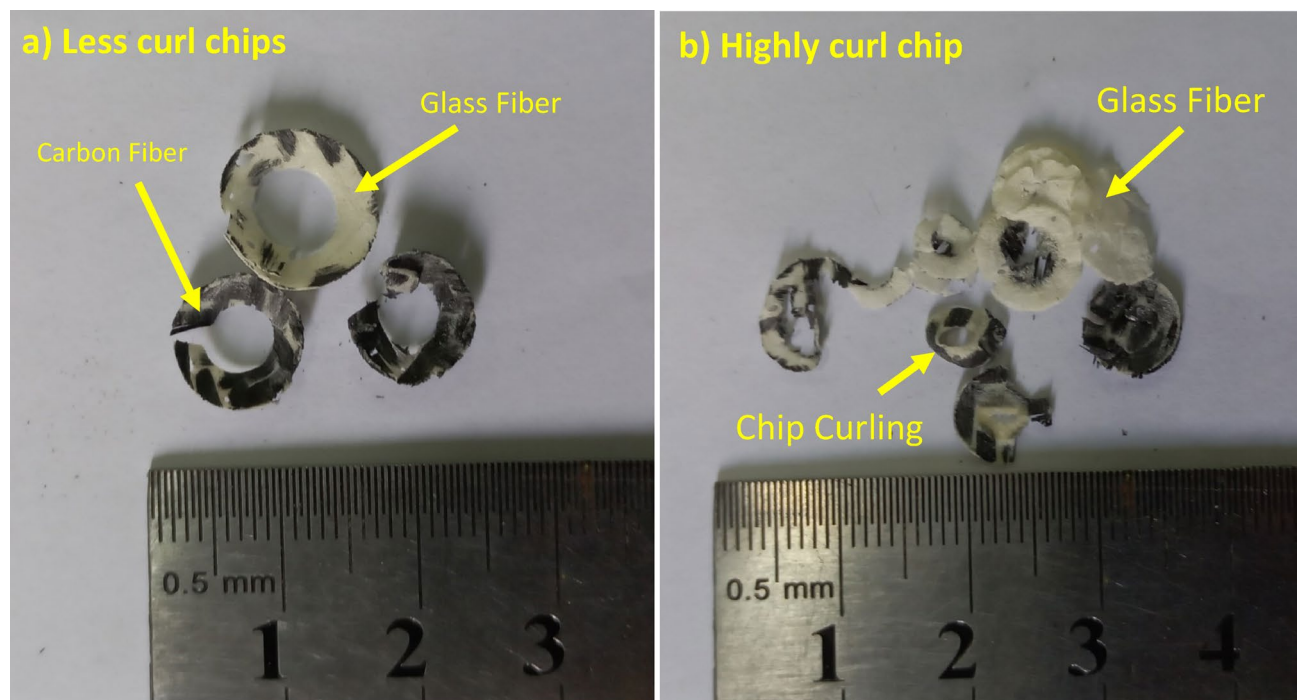


Fig. 10. (a) Less curl chips from LM geometry (b) Highly curl chips from GT Geometry.

tool life. Conversely, the GT geometry provides a lower depth and shallow angle for rigid HFRP/Al sandwich composites through which chips can easily flow and cause less rubbing with the tool and hole wall; therefore, the GT geometry is more suitable for machining HFRP/Al sandwich materials.

Authors claim is further supported in Figs. 10(a) and (b) which clearly shows longer and less curl chips for the LM geometry, which makes it difficult for chips to pass through the same flutes compared to the highly curl chips produced in the case of the GT geometry. From the literature, it was concluded that continuous chip

streaming is one of the mechanisms that trigger tool wear³². According to Seker U et al.³³ their findings were consistent with the observation that smaller chips tend to produce stronger chip-breaking. The accumulation of unbroken chips from the workpiece poses a negative impact on both tool wear and worker safety²³. Sahu et al.³⁴ demonstrated this by examining the drilling of a 1018 steel workpiece using two drills: one with a grooved chip breaker and the other without. They discovered a 55% improvement in tool life when using chip breaker-type drilling, because the grooved type chip breaker produced smaller chips, making the evacuation process more efficient. This results in a reduction in force and an increase in drill life.

Optical micrographs of the inserts are shown in Fig. 11 for the extended tool life experiments. The micrographs were obtained at a magnification of X70 using CMM. Uniform wear was observed at the flank side of the cutting tool, whereas minor chipping was observed in Tests 1E using the GT geometry. However, this minor chipping was ignored because it was below the value of the maximum wear criterion of 150 μm .

Prior to starting any experiment, images of cutting inserts were captured using scanning electron microscope (SEM) to verify the consistency of the edges and are shown in Fig. 12. Figure 13 presents scanning electron microscope (SEM) micrographs of the GT wiper insert after 120 holes at FR of 0.08 mm/rev. The images reveal uniform wear on the flank side of the cutting insert. Chipping is evident at the rake face and cutting nose of the insert, while minor material adhesion is observed on the rake face. Figure 14 displays the SEM micrograph of the LM central insert after 120 holes. The images show uniform wear on the flank of the insert. Overall, lower wear for the central insert was observed compared to the wiper insert.

Diametric error for extended tests

The results for Tests 1E and 3E, which used geometries GT and LM and a feed of 0.08 mm/rev, are depicted in Fig. 15. The results demonstrated that the GT geometry exhibited lower diametric errors, while the LM geometry displayed higher diametric errors. This difference can be attributed to the continuous chips produced with the LM geometry which are more likely to become entangled with the tool holder and rub against the drilled hole, causing it to enlarge compared with the nominal hole size. Moreover, owing to the rubbing of chips, heat is produced on the internal surface of hole which results in thermal expansion. Xu et al.³⁵ also studied the geometrical accuracy of holes while comparing the dry and minimum quantity lubrication (MQL) drilling of CFRP/Ti6Al4V stacks. It was observed that elevating either FR or CS typically led to an increase in hole diameter. In addition, holes drilled in a dry environment lead to surfaces that are noticeably rougher, exhibiting a large number of machining-induced defects. The diameters of the holes are consistently significantly different from the intended size, mainly because of the increase in cutting vibration as the thickness of the uncut composite decreases, particularly when the drill edges move from the entry to the exit side. An et al.³⁶ also

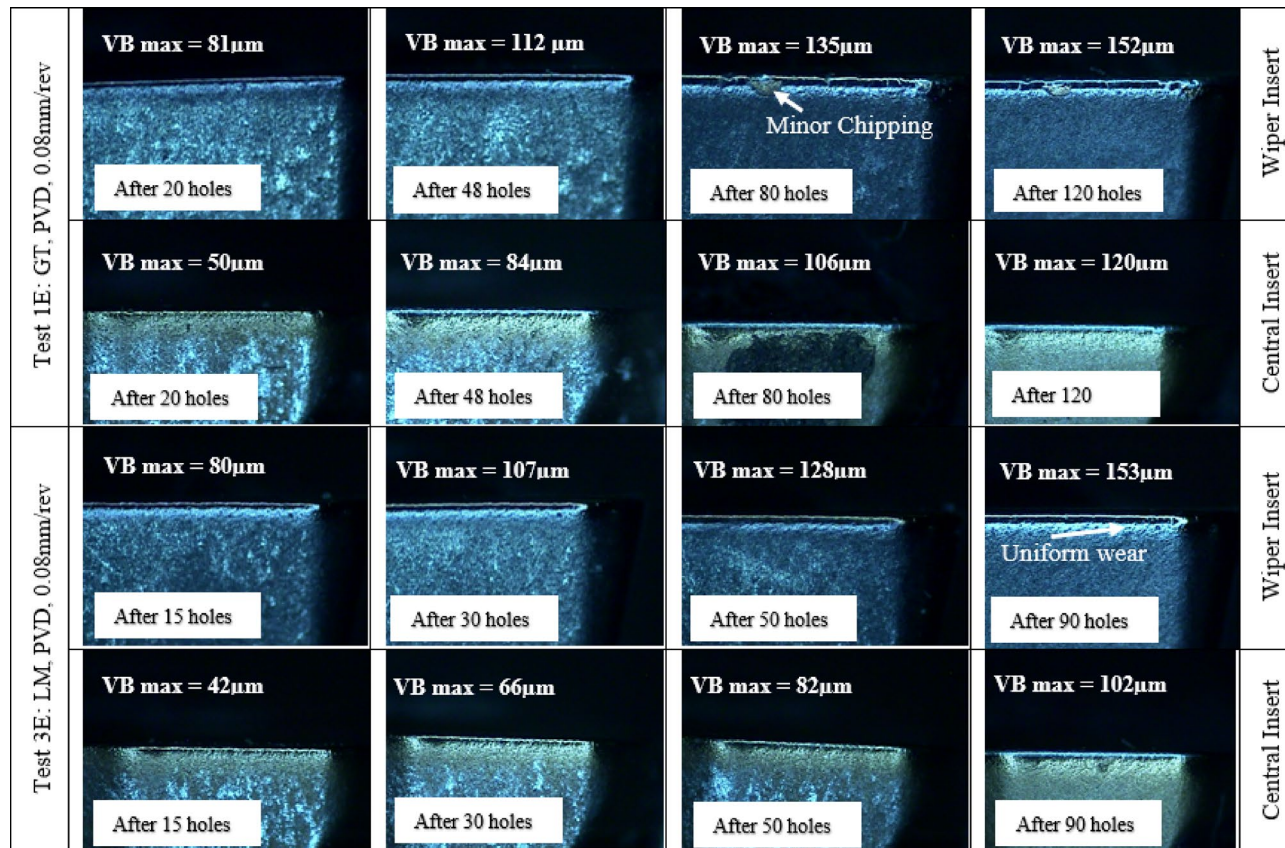


Fig. 11. Tool Wear Progression Images.

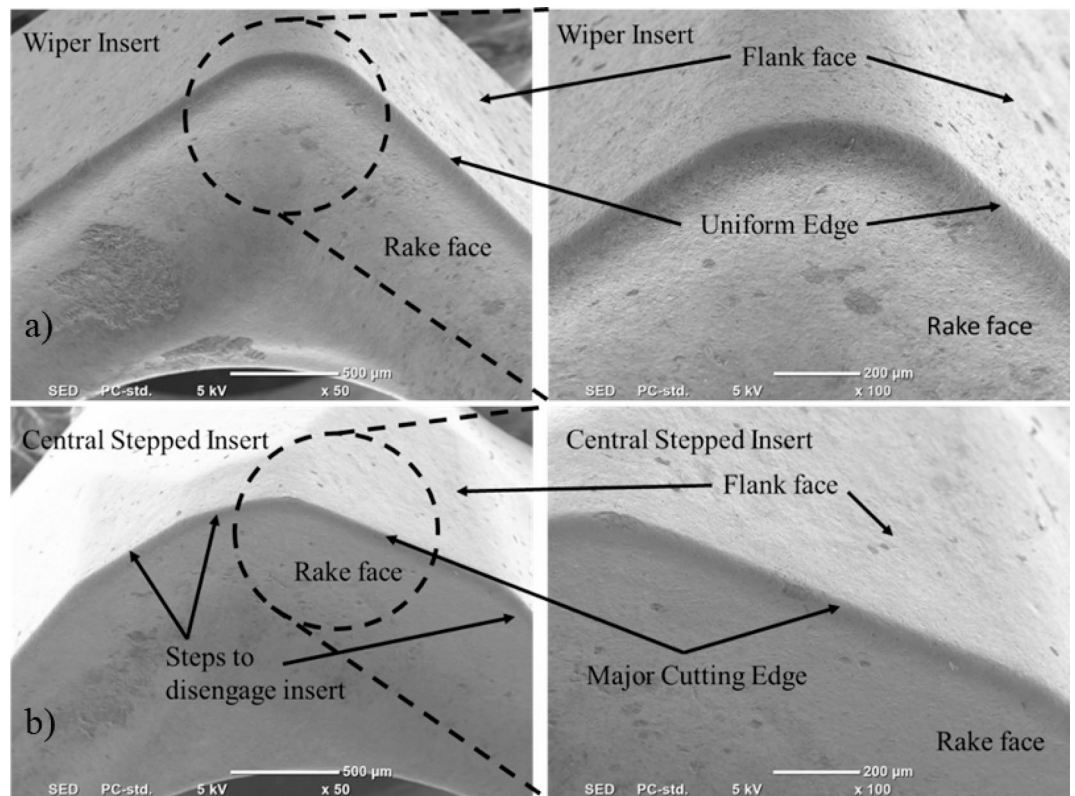


Fig. 12. SEM images of new cutting edge of (a) wiper and (b) central insert.

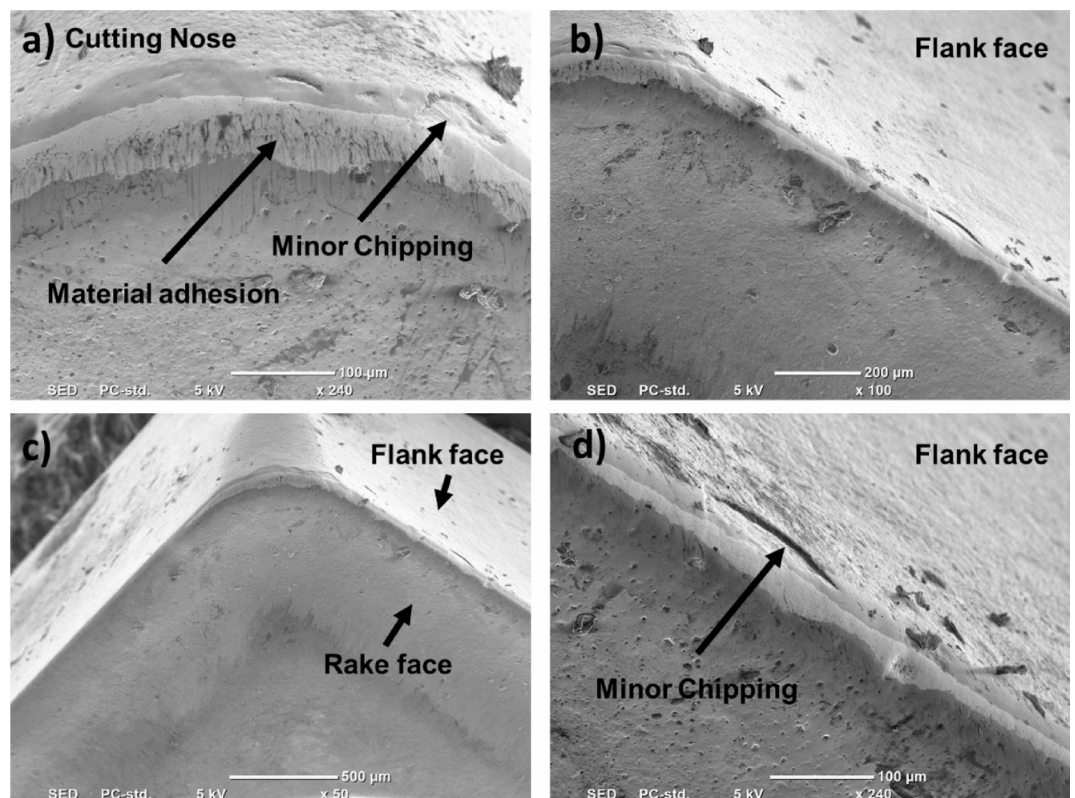


Fig. 13. SEM Images of GT geometry wiper insert after 120 holes at FR of 0.08 mm/rev.

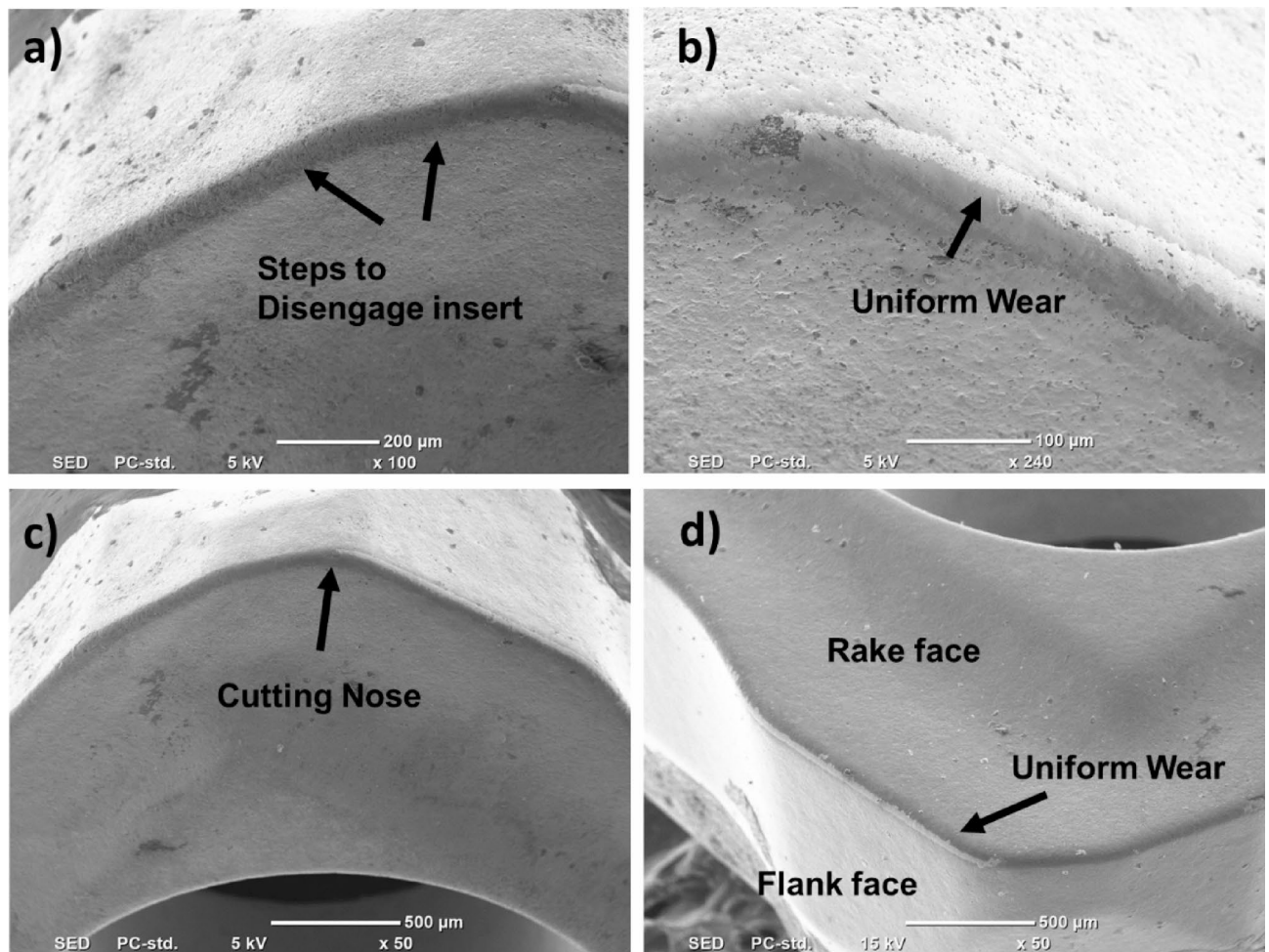


Fig. 14. SEM Images of LM geometry central insert after 120 holes at *FR* of 0.08 mm/rev.

studied the drilling of CFRP-Ti stacks and observed the similar results. Wang et al.,³⁷ studied the hole quality of CFRP/aluminum stacks using diamond coated tools and reported an increasing trend in the diametric error with respect to the *FR*. The higher diametric error at higher *FR* was attributed to the cutting vibration and the instability of the cutting condition as the *FR* increased.

Delamination factor for extended tests

Evaluating and contrasting the degree of delamination resulting from drilling of laminated composites is critical for assessing their quality and performance. Delamination can degrade the structural integrity of these materials, leading to potential issues such as failure or reduced lifespans. The nominal and maximum diameters for Tests 1E and 3E are shown in Fig. 16; Table 4, and the results of the delamination factors with respect to the number of holes are presented in Fig. 17.

The result indicates that, in terms of a lower delamination factor, the GT geometry performs better than the LM geometry. It was previously noted that the use of LM geometry resulted in the formation of longer chips with a lesser curl. These chips are prone to slight entanglement with the tool holder and exhibit rubbing against the surface of the hole, potentially increasing the delamination factor. When using the GT geometry, higher curls and broken chips were observed, which led to a lower delamination factor. According to Fu-ji Wang et al.³⁸, similar outcomes were obtained when drilling CFRP/Al stacks and it was reported that using a conventional drill, difficult evacuation of the continuous chip and scratching damages were observed due to the accumulation of wrapped chips on the drill bit while drilling. Whereas, the chip breaker drills were able to break the chips more effectively into a favorable size, which, in turn, increased the overall hole quality at the entrance and the exist of drilled holes. Furthermore, the quality of the hole edge noticeably declined, resulting in an increased number of produced holes, particularly at the hole exit. The occurrence of this phenomenon can be attributed to the deterioration of the drill edge sharpness, leading to an augmentation of the thrust forces. The tool wear for the LM geometry was higher than that for the GT geometry, resulting in a higher delamination factor for the same number of holes. This outcome was also observed by Chen³⁹, who found that the delamination factor is proportional to the flank wear of the drill bit. The decline in drill-edge sharpness causes an increase in the thrust forces, which results in a higher delamination factor.

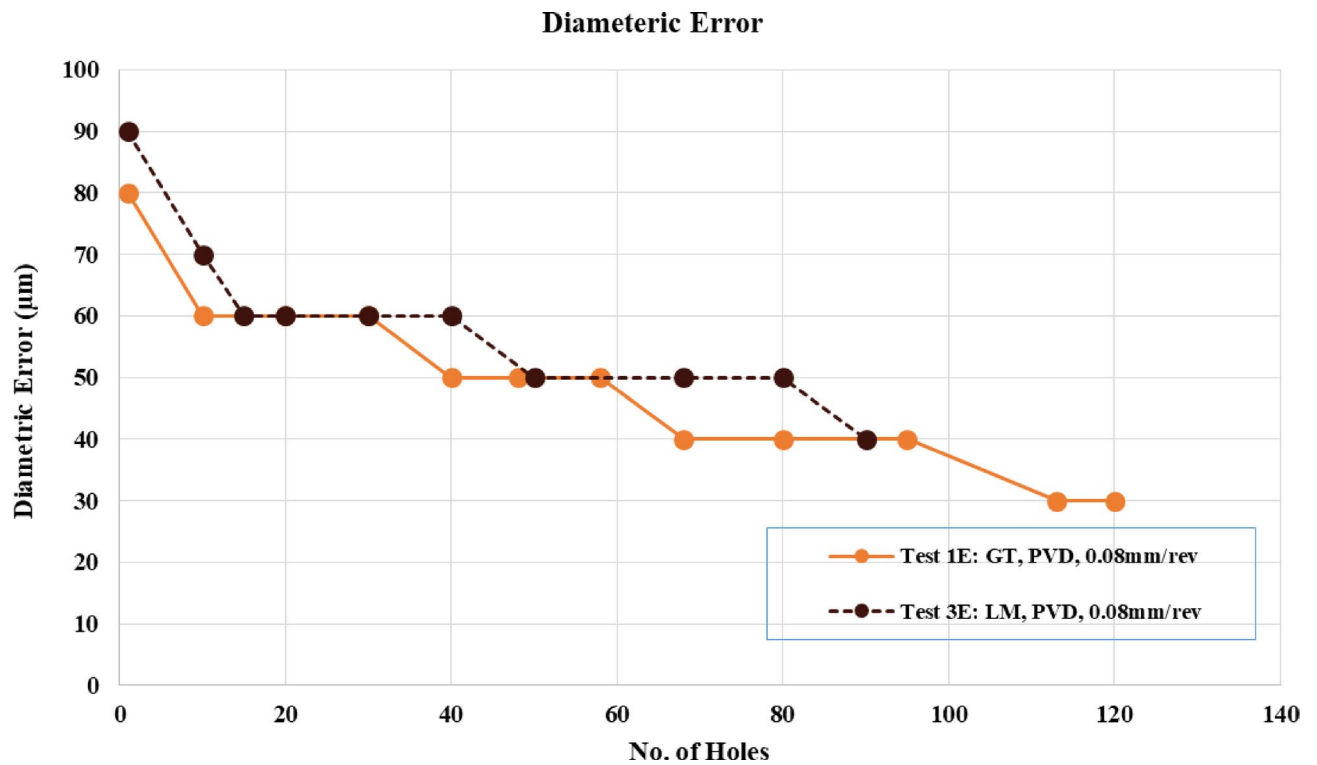


Fig. 15. Diametric error for Extended tests.

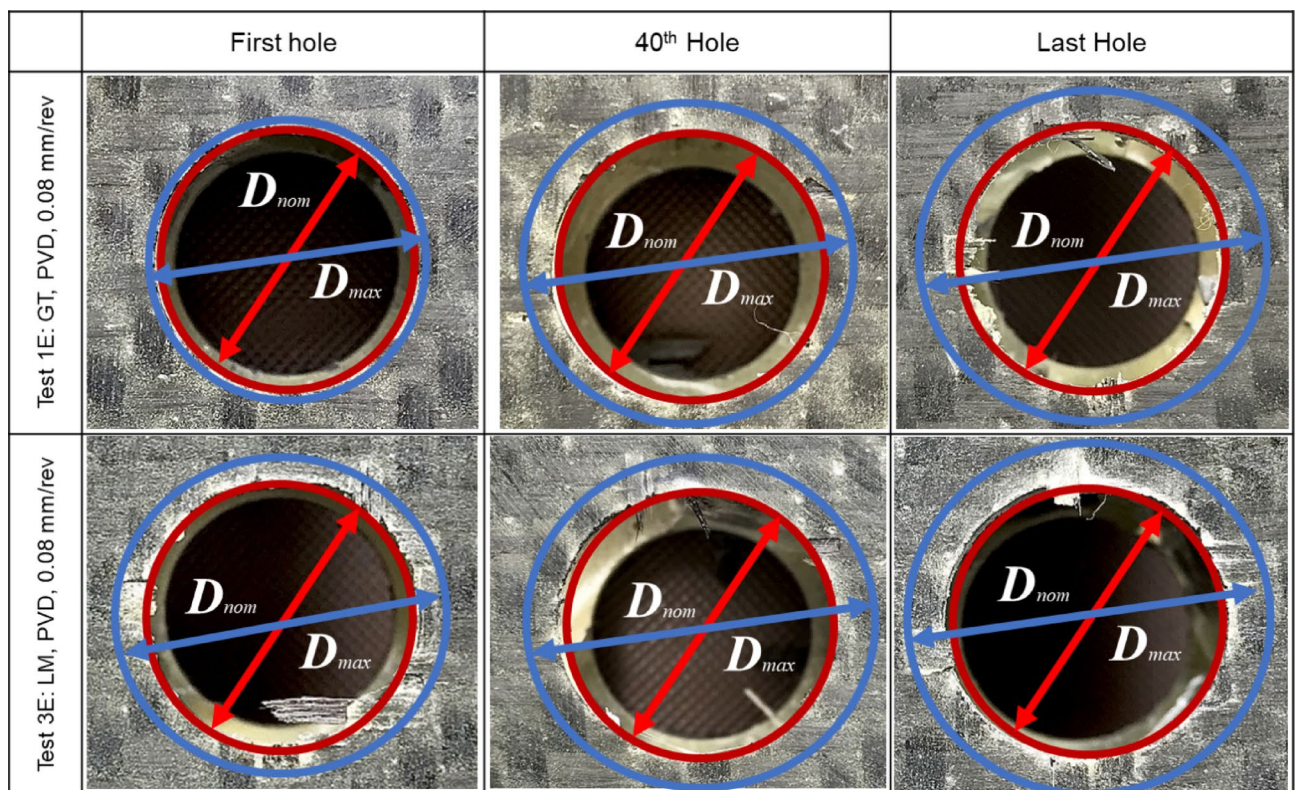


Fig. 16. Nominal Diameter and Maximum Diameter at bottom side of Tests 1E and 3E.

| Test 1E: GT, PVD, 0.08 mm/rev | | Test 3E: LM, PVD, 0.08 mm/rev | |
|-------------------------------------|------------------|-------------------------------------|------------------|
| Hole no | D _{max} | Hole no | D _{max} |
| 10 | 14.2 | 10 | 14.18 |
| 60 | 14.28 | 30 | 14.25 |
| 90 | 14.32 | 70 | 14.45 |
| 120 | 14.33 | 90 | 14.56 |

Table 4. Maximum measured diameter for tests 1E and 3E.

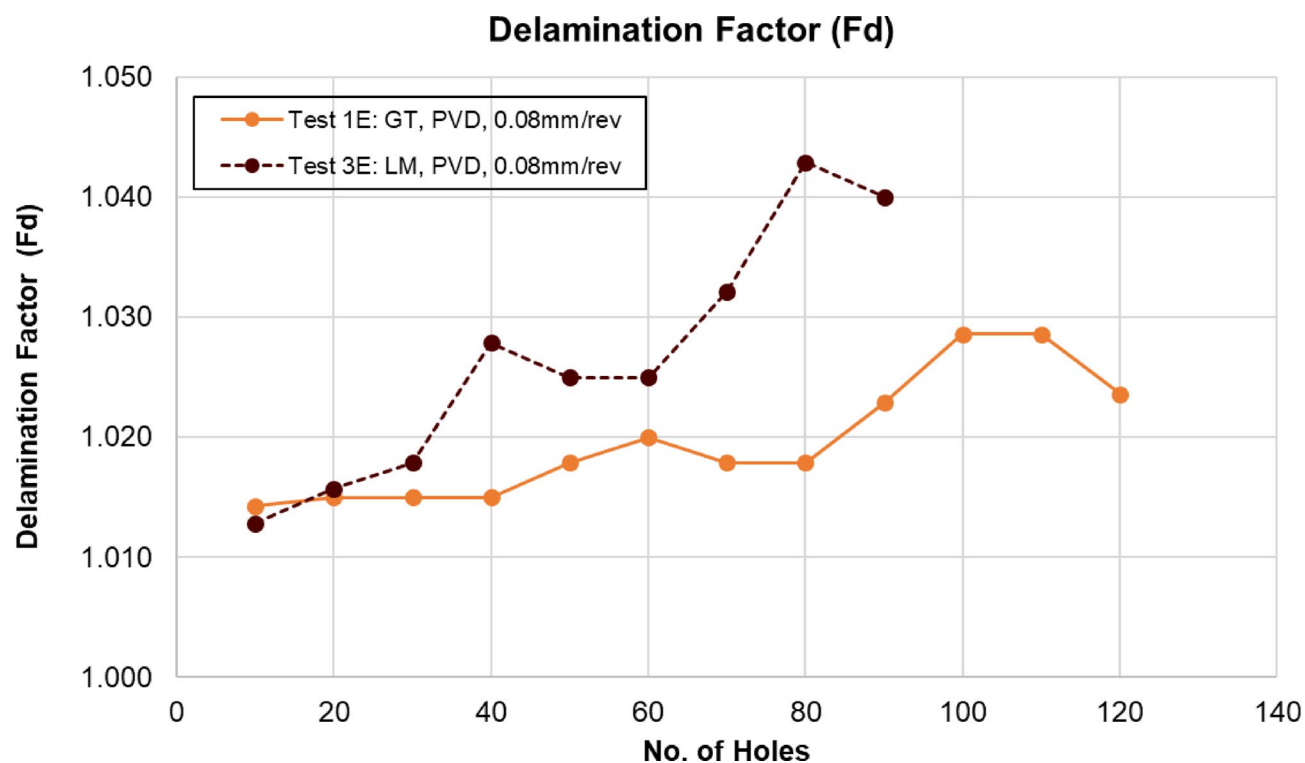


Fig. 17. Delamination factor for Extended tests.

Conclusions

The study evaluated central stepped inserts combined with peripheral wiper inserts for drilling fire-retardant HFRP/Al sandwich composites in two phases. Phase I involved drilling ten holes at feed rates of 0.08 mm/rev and 0.06 mm/rev, as well as a high feed rate of 0.16 mm/rev. The high feed rate resulted in severe tool wear, increased diametric error, and extensive delamination defects, such as burrs and tears. Consequently, a feed rate of 0.08 mm/rev was selected for the Phase II experimentation and the following conclusions were drawn:

- The GT geometry exhibited a significant enhancement in tool life, achieving 120 drilled holes, a 33.3% improvement compared to the LM configuration, which completed 90 holes. This superior performance is attributed to the GT geometry's robust design, which facilitated improved chip flow and effective chip curling, thereby enhancing overall drilling efficiency.
- The GT geometry demonstrated a diametric error of 80 μ m, representing an 11% reduction compared to the LM geometry. Additionally, the diametric error for the GT geometry improved progressively during the drilling process, starting at 80 μ m for the first hole and decreasing to 30 μ m for the last hole representing 62% reduction in error with time.
- In addition, the GT and LM geometries exhibit negligible disparities in the delamination factor at the outset. However, as the number of holes increased, the GT geometry exhibited lower values of delamination factor than the LM geometry.

Data availability

Data Availability Statement: The datasets used and analyzed during the current study are available from the corresponding author upon reasonable request.

Received: 19 July 2024; Accepted: 22 May 2025

Published online: 27 May 2025

References

1. Tan, C. L., Azmi, A. I. & Muhammad, N. Surface roughness analysis of carbon/glass hybrid polymer composites in drilling process based on Taguchi and response surface methodology. *Adv. Mater. Res.* **1119** <https://doi.org/10.4028/www.scientific.net/amr.1119.622> (2015).
2. Yu, J., Pan, Z., Ye, W., Li, Q. & Wu, Z. Dynamic temperature field and drilling damage mechanism of plain woven carbon/glass hybrid composites. *Compos. Struct.* <https://doi.org/10.1016/j.compstruct.2022.116375> (2023).
3. Li, N., Li, Y., Zhou, J., He, Y. & Hao, X. Drilling delamination and thermal damage of carbon nanotube/carbon Fiber reinforced epoxy composites processed by microwave curing. *Int. J. Mach. Tools Manuf.* <https://doi.org/10.1016/j.ijmachtools.2015.06.005> (2015).
4. Xu, J., Li, C., Chen, M. & Ren, F. A. Comparison between vibration assisted and conventional drilling of CFRP/Ti6Al4V stacks. *Mater. Manuf. Processes.* **34**, 1182–1193. <https://doi.org/10.1080/10426914.2019.1615085> (2019).
5. Xu, J., Li, C., Chen, M., Mansori, E., Paulo Davim, J. & M. & On the analysis of temperatures, surface morphologies and tool wear in drilling CFRP/Ti6Al4V stacks under different cutting sequence strategies. *Compos. Struct.* **234** <https://doi.org/10.1016/j.compsstruct.2019.111708> (2020).
6. Grillo, T., Paulo, R., Silva, C. & Davim, J. Experimental delamination analyses of CFRPs using different Drill geometries. *Compos. Part. B Eng.* **45**, 1344–1350. <https://doi.org/10.1016/j.compositesb.2012.07.057> (2013).
7. Braiek, S. et al. Drilling of filament wound hybrid composite tubes: an experimental study. *Compos. Struct.* **308**, 116686. <https://doi.org/10.1016/j.compstruct.2023.116686> (2023).
8. Boughdiri, I., Mabrouki, T., Zitoun, R., Giasin, K. & Ameer, M. F. 3D Macro-Mechanical FE simulation for GLARE® drilling with experimental validation. *Compos. Struct.* **304**, 116458. <https://doi.org/10.1016/j.compstruct.2022.116458> (2022).
9. Sourd, X., Giasin, K., Zitoun, R., Salem, M. & Lupton, C. Multi-Scale analysis of the damage and contamination in abrasive water jet drilling of GLARE fibre metal laminates. *J. Manuf. Process.* **84**, 610–621. <https://doi.org/10.1016/j.jmapro.2022.10.023> (2022).
10. Ge, J. et al. Towards Understanding the hole making performance and chip formation mechanism of thermoplastic carbon fibre/polyetherketoneketone composite. *Compos. Part. B Eng.* **234**, 109752. <https://doi.org/10.1016/j.compositesb.2022.109752> (2022).
11. Ge, J. et al. Multi-objective optimization of thermoplastic CF/PEKK drilling through a hybrid method: an approach towards sustainable manufacturing. *Compos. Part. Appl. Sci. Manuf.* **167**, 107418. <https://doi.org/10.1016/j.compositesa.2022.107418> (2023).
12. Ge, J. et al. Temperature-dependent cutting physics in orthogonal cutting of carbon fibre reinforced thermoplastic (CFRTP) composite. *Compos. Part. Appl. Sci. Manuf.* **176**, 107820. <https://doi.org/10.1016/j.compositesa.2023.107820> (2023).
13. Ge, J. et al. Temperature field evolution and Thermal-mechanical interaction induced damage in drilling of thermoplastic CF/PEKK – A comparative study with thermoset CF/Epoxy. *J. Manuf. Process.* **88**, 167–183. <https://doi.org/10.1016/j.jmapro.2023.01.042> (2023).
14. Sharma, A. P., Khan, S. H. & Parameswaran, V. Experimental and numerical investigation on the Uni-Axial tensile response and failure of Fiber metal laminates. *Compos. Part. B Eng.* **125**, 259–274. <https://doi.org/10.1016/j.compositesb.2017.05.072> (2017).
15. Anjang, A. et al. Post-Fire mechanical properties of sandwich composite structures. *Compos. Struct.* **132**, 1019–1028. <https://doi.org/10.1016/j.compstruct.2015.07.009> (2015).
16. Zhu, S., Wu, S., Fu, Y. & Guo, S. Prediction of particle-reinforced composite material properties based on an improved Halpin–Tsai model. *AIP Advances*, **14**(4), 045339. <https://doi.org/10.1063/5.0206774> (2024).
17. Javadi, A., Ashraf, H. T., Mustaghees, M. & Khalid, A. Fire-retardant carbon/glass Fabric-reinforced epoxy sandwich composites for structural applications. *Polym. Compos.* **42**, 45–56. <https://doi.org/10.1002/pc.25806> (2020).
18. Ji, R., Liu, Y., Zhang, Y. & Wang, F. Machining performance of silicon carbide ceramic in end electric discharge milling. *International Journal of Refractory Metals and Hard Materials*, **29**(1), 117–122. <https://doi.org/10.1016/j.ijrmhm.2010.09.001> (2011).
19. Anwar, S., Khan, N. A., Khan, S. A. & Raza, S. F. One-Step High-Speed finish drilling of inconel 718 Superalloy via novel inserts. *Processes* **11**, 752. <https://doi.org/10.3390/pr11030752> (2023).
20. Sun, J., Zhang, Z., Zhang, Y., Zhang, X., Guo, J., Fu, Q. & Wu, L. High-temperature ablation resistance prediction of ceramic coatings using machine learning. *Journal of the American Ceramic Society*, **108**(1), e20136. <https://doi.org/10.1111/jace.20136> (2025).
21. Afzal, M. Z., Khan, S. A., Khan, A. M., Saleem, M. Q. & Anwar, S. Wear behavior of novel CVD-Coated wiper inserts' with various Chip-Breakers and resulting surface integrity during dry drilling of Ti-6Al-4V. *Tribol Int.* **202**, 110323. <https://doi.org/10.1016/j.triboint.2024.110323> (2024).
22. Website <https://www.youtube.com/@sandvikcoromant> Accessed on 18th January (2025).
23. Gürbüz, H., Kafkas, F. & Şeker, U. AISI 316L Çelikinin İşlenmesinde kesici Takım kesici Kenar formu ve Talaş Kırıcı Formların Kesme kuvvetleri ve Yüzey Pürüzlülüğü Üzerine Etkisi. *Batman Üniv Yaşam Bilim Derg* **1**, 173–184. <https://doi.org/10.17341/gazimmfd.454386>
24. Lotfi, M., Akhavan Farid, A. & Soleimanimehr, H. The effect of chip breaker geometry on chip shape, bending moment, and cutting force: FE analysis and experimental study. *Int. J. Adv. Manuf. Technol.* **78**, 917–925. <https://doi.org/10.1007/s00170-014-6676-8> (2014).
25. Ji, R. et al. Influence of dielectric and machining parameters on the process performance for electric discharge milling of SiC ceramic. *The International Journal of Advanced Manufacturing Technology*, **59**(1), 127–136. <https://doi.org/10.1007/s00170-011-3493-1> (2012).
26. Khan, S. A. et al. Wear performance of modified inserts in hard turning of AISI D2 steel: A concept of One-step sustainable machining. *J. Manuf. Process.* **60**, 457–469. <https://doi.org/10.1016/j.jmapro.2020.10.052> (2020).
27. Babu, J. et al. (ed Davim, J.) Assessment of delamination in composite materials: A review. *Proc. Inst. Mech. Eng. Part. B J. Eng. Manuf.* **230** 1990–2003 <https://doi.org/10.1177/0954405415619343> (2016).
28. Fan, T. et al. Nucleation and growth of L12-Al3RE particles in aluminum alloys: A first-principles study. *Journal of Rare Earths*, **41**(7), 1116–1126. <https://doi.org/10.1016/j.jre.2022.05.018> (2023).
29. Rajkumar, G. M., Bhardwaj, D., Kannan, C., Oyyaravelu, R. & Balan, A. S. S. Effect of chilled air on delamination, induced vibration, burr formation and surface roughness in CFRP drilling: A comparative study. *Mater. Res. Express.* **6**, 035305. <https://doi.org/10.1088/2053-1591/aaf47d> (2018).
30. Davim, J. & Reis, P. Study of delamination in drilling carbon Fiber reinforced plastics (CFRP) using design experiments. *Compos. Struct.* **59**, 481–487. [https://doi.org/10.1016/s0263-8223\(02\)00257-x](https://doi.org/10.1016/s0263-8223(02)00257-x) (2003).
31. Durão, L. M. P., Tavares, J. M. R., de Albuquerque, V. H. C. & Gonçalves, D. J. Damage evaluation of drilled carbon/epoxy laminates based on area assessment methods. *Compos. Struct.* **96**, 576–583. <https://doi.org/10.1016/j.compstruct.2012.08.003> (2013).
32. Zou, B. et al. Impact of tunneling parameters on disc cutter wear during rock breaking in transient conditions. *Wear*, **560–561**, 205620. <https://doi.org/10.1016/j.wear.2024.205620> (2025).
33. Şeker, U. Takım Tasarımı Ders Notları. Ankara (1997).
34. Sahu, S. K., Ozdoganlar, B., DeVor, R. E. & Kapoor, S. G. Effect of Groove-Type chip breakers on twist Drill performance. *Int. J. Mach. Tools Manuf.* **43**, 617–627. [https://doi.org/10.1016/s0890-6955\(02\)00303-6](https://doi.org/10.1016/s0890-6955(02)00303-6) (2003).

35. Xu, J., Ji, M., Chen, M. & Ren, F. Investigation of minimum quantity lubrication effects in drilling CFRP/Ti6Al4V stacks. *Mater. Manuf. Processes*. **34**, 1401–1410. <https://doi.org/10.1080/10426914.2019.1661431> (2019).
36. An, Q., Dang, J., Li, J., Wang, C. & Chen, M. Investigation on the cutting responses of CFRP/Ti stacks: with special emphasis on the effects of drilling sequences. *Compos. Struct.* **253**, 112794. <https://doi.org/10.1016/j.compstruct.2020.112794> (2020).
37. Wang, C. et al. Drilling temperature and hole quality in drilling of CFRP/Aluminum stacks using diamond coated Drill. *Int. J. Precis Eng. Manuf.* **16**, 1689–1697. <https://doi.org/10.1007/s12541-015-0222-y> (2015).
38. Wang, F. J. et al. Novel Chip-Breaking structure of step Drill for drilling damage reduction on CFRP/Al stack. *J. Mater. Process. Technol.* **291**, 117033. <https://doi.org/10.1016/j.jmatprotec.2020.117033> (2021).
39. Chen, W. C. Some experimental investigations in the drilling of carbon Fiber-Reinforced plastic (CFRP) composite laminates. *Int. J. Mach. Tools Manuf.* **37**, 1097–1108. [https://doi.org/10.1016/s0890-6955\(96\)00095-8](https://doi.org/10.1016/s0890-6955(96)00095-8) (1997).

Acknowledgements

The Authors acknowledge the University of Engineering and Technology, Lahore, Pakistan for the provision of experimentation. The authors appreciate the support from Researchers Supporting Project number (RSP-D2024R702), King Saud University, Riyadh, Saudi Arabia.

Author contributions

M. Z. A, S. A. K, M. U. F., A. J., S. A. wrote the main manuscript text and M. Z. A, S. A. K, M. U. F., A. J., S. A., A. A.A prepared figures. All authors reviewed the manuscript.

Declarations

Consent for publication

All authors agreed upon the current version of the submission for publication.

Competing interests

The authors declare no competing interests.

Conflict of interest

The authors declare no conflict of interest.

Additional information

Correspondence and requests for materials should be addressed to M.U.F. or A.A.A.

Reprints and permissions information is available at www.nature.com/reprints.

Publisher's note Springer Nature remains neutral with regard to jurisdictional claims in published maps and institutional affiliations.

Open Access This article is licensed under a Creative Commons Attribution-NonCommercial-NoDerivatives 4.0 International License, which permits any non-commercial use, sharing, distribution and reproduction in any medium or format, as long as you give appropriate credit to the original author(s) and the source, provide a link to the Creative Commons licence, and indicate if you modified the licensed material. You do not have permission under this licence to share adapted material derived from this article or parts of it. The images or other third party material in this article are included in the article's Creative Commons licence, unless indicated otherwise in a credit line to the material. If material is not included in the article's Creative Commons licence and your intended use is not permitted by statutory regulation or exceeds the permitted use, you will need to obtain permission directly from the copyright holder. To view a copy of this licence, visit <http://creativecommons.org/licenses/by-nc-nd/4.0/>.

© The Author(s) 2025